

## Experimental Verification of $\text{PbBi}_2\text{Te}_4$ as a 3D Topological Insulator

K. Kuroda,<sup>1</sup> H. Miyahara,<sup>1</sup> M. Ye,<sup>1</sup> S. V. Eremeev,<sup>2,3</sup> Yu. M. Koroteev,<sup>2,3</sup> E. E. Krasovskii,<sup>4,5,6</sup> E. V. Chulkov,<sup>4,5</sup> S. Hiramoto,<sup>1</sup> C. Moriyoshi,<sup>1</sup> Y. Kuroiwa,<sup>1</sup> K. Miyamoto,<sup>7</sup> T. Okuda,<sup>7</sup> M. Arita,<sup>7</sup> K. Shimada,<sup>7</sup> H. Namatame,<sup>7</sup> M. Taniguchi,<sup>1,7</sup> Y. Ueda,<sup>8</sup> and A. Kimura<sup>1,\*</sup>

<sup>1</sup>Graduate School of Science, Hiroshima University, 1-3-1 Kagamiyama, Higashi-Hiroshima 739-8526, Japan

<sup>2</sup>Institute of Strength Physics and Materials Science, 634021, Tomsk, Russia

<sup>3</sup>Tomsk State University, 634050, Tomsk, Russia

<sup>4</sup>Departamento de Física de Materiales UPV/EHU 20080 San Sebastián/Donostia, Basque Country, Spain and Centro de Física de Materiales CFM 20080 San Sebastián/Donostia, Basque Country, Spain and Centro Mixto CSIC-UPV/EHU, 20080 San Sebastián/Donostia, Basque Country, Spain

<sup>5</sup>Donostia International Physics Center (DIPC), 20018 San Sebastián/Donostia, Basque Country, Spain

<sup>6</sup>IKERBASQUE, Basque Foundation for Science, 48011 Bilbao, Spain

<sup>7</sup>Hiroshima Synchrotron Radiation Center, Hiroshima University, 2-313 Kagamiyama, Higashi-Hiroshima 739-0046, Japan

<sup>8</sup>Kure National College of Technology, Agaminami 2-2-11, Kure 737-8506, Japan

(Received 7 November 2011; published 15 May 2012)

The experimental evidence is presented of the topological insulator state in  $\text{PbBi}_2\text{Te}_4$ . A single surface Dirac cone is observed by angle-resolved photoemission spectroscopy with synchrotron radiation. Topological invariants  $\mathbb{Z}_2$  are calculated from the *ab initio* band structure to be 1;(111). The observed two-dimensional isoenergy contours in the bulk energy gap are found to be the largest among the known three-dimensional topological insulators. This opens a pathway to achieving a sufficiently large spin current density in future spintronic devices.

DOI: 10.1103/PhysRevLett.108.206803

PACS numbers: 73.20.-r, 71.20.-b, 75.70.Tj, 79.60.-i

Topological insulators (TIs) have recently emerged as a new state of quantum matter, which are distinguished from conventional insulators by having a surface state with a massless Dirac dispersion in the bulk energy gap. The spin orientation of the topological surface state is locked with its crystal momentum, resulting in a helical spin texture. This new state can be classified by so-called  $\mathbb{Z}_2$  topological invariants [1,2]. Generally, the massless Dirac cone can be created at an interface of two materials: a topological and an ordinary insulator. The unique properties of topological surface electrons provide a fertile ground to realize new electronic phenomena, such as a magnetic monopole arising from the topological magneto-electric effect and Majorana fermions at the interface with a superconductor [3,4]. Owing to time-reversal symmetry, topological surface states are protected from backscattering in the presence of a weak perturbation, which is required for the realization of dissipationless spin transport without external magnetic fields in novel quantum devices [5,6].

A number of materials that hold spin-polarized surface Dirac cones have been intensively studied, such as  $\text{Bi}_{1-x}\text{Sb}_x$  [7,8],  $\text{Bi}_2\text{Te}_3$  [9,10],  $\text{Bi}_2\text{Se}_3$  [11–14], and thallium-based compounds [15–21]. Among them,  $\text{Bi}_2\text{Se}_3$  has been regarded as one of the most promising candidates for potential applications in ultralow power consumption quantum devices that can work stably at room temperature due to a sufficiently large bulk energy gap. Although significant efforts have been made toward spintronic applications, the surface contribution to conduction was hardly observed even at low bulk carrier density

[22–24]. This motivates the search for new topological insulators with higher density of spin-polarized Dirac fermions.

Recently, some of the Pb-based ternary chalcogenides have been proposed as three-dimensional (3D) topological insulators [25–27]. The present study is focused on  $\text{PbBi}_2\text{Te}_4$ , which has the simplest crystal structure among them. The crystal is composed of seven-layer blocks with the atomic layer sequence Te-Bi-Te-Pb-Te-Bi-Te (see Fig. S1(a) of the Supplemental Material (SM) [28]) [29]. The theoretical analysis of Ref. [27] indicates that this compound is a 3D topological insulator. In this Letter, we report the first experimental evidence of the topological surface state in  $\text{PbBi}_2\text{Te}_4$  by angle-resolved photoemission spectroscopy (ARPES). We establish that the size of the two-dimensional isoenergy contour, which is proportional to the surface carrier density, is the largest among the known 3D topological insulators. Thus,  $\text{PbBi}_2\text{Te}_4$  can be counted as one of the most promising candidates for realizing a large spin current density in future spintronic devices.

A single crystalline sample of  $\text{PbBi}_2\text{Te}_4$  was grown by the standard procedure using Bridgman method (see SM [28] for more details). For ARPES measurement the samples were *in situ* cleaved along the basal plane. Photoemission experiment was performed with synchrotron radiation at the linear undulator beam line (BL1) and the helical undulator beamline (BL9A) of Hiroshima Synchrotron Radiation Center (HiSOR). The ARPES spectra were acquired with a hemispherical photoelectron analyzer (VG-SCIENTA R4000) at 17 K. The overall

energy and angular resolutions were set to 10–20 meV and  $0.3^\circ$ , respectively.

Figure 1(a) shows the ARPES energy dispersion curve along the  $\bar{\Gamma}\bar{K}$  line of the surface Brillouin zone [see SM [28], Fig. S1(b)] measured at  $h\nu = 7.5$  eV. The parabolic band with the energy minimum at the binding energy of  $E_B = 200$  meV is seen to exhibit a rather strong photo-emission intensity near the  $\bar{\Gamma}$  point. The position of the energy minimum does not change with the photon energy [see SM [28], Figs. S2(a) and S2(b)], which confirms the two-dimensional nature of this electronic state. More importantly, a linearly dispersing feature, i.e., the Dirac cone (DC) with the crossing point at  $E_B = 470$  meV is observed.

Figures 1(b) and 1(c) summarize the constant energy contours (i) and their second derivatives (ii) in the  $\mathbf{k}_{\parallel}$  range  $-0.3 \text{ \AA}^{-1} \leq k_x, k_y \leq +0.3 \text{ \AA}^{-1}$  from  $E_B = 470$  meV (Dirac point) to 0 (Fermi level) at  $h\nu = 7.5$  and 10 eV, respectively. With  $h\nu = 10$  eV we find at the Dirac point energy six ellipses oriented along  $\bar{\Gamma}\bar{M}$  in addition to the pointlike feature at the  $\bar{\Gamma}$  point for the Dirac state. On the other hand, the elliptical contours are much weaker at  $h\nu = 7.5$  eV, signifying a strong matrix elements effect. In going away from the Dirac point, the sole hexagonally shaped contour is observed down to  $E_B = 290$  meV and at smaller binding energies another state becomes enclosed

inside the Dirac cone (starting with  $E_B = 260$  meV). It is interpreted as the onset of the bulk conduction band (BCB) because the shape of the inner contours considerably depends on the photon energy, see Figs. 1(b) and 1(c). Below  $E_B = 160$  meV the Dirac cone further deforms and practically merges into the BCB. In the map measured with  $h\nu = 10$  eV the hexagonal Fermi surface of the Dirac cone encloses two large and one small triangular shaped surfaces centered at  $\bar{\Gamma}$ . At  $h\nu = 7.5$  eV the shape of the inner Fermi surfaces strongly changes and becomes very complicated, which is consistent with a bulk state (see Fig. S4 of SM [28]). The size of the energy gap is estimated as 230 meV as shown in the 3D map for  $h\nu = 10$  eV [Fig. 1(d)]. Such a large energy gap is beneficial for a high stability of the spin current conductance at room temperature. Figure 1(d) illustrates a high anisotropy of the bulk valence band (BVB): the valence band maximum in the  $\bar{M}\bar{\Gamma}\bar{M}$  line is at  $E_B = 490$  meV ( $k_{\parallel} = \pm 0.3 \text{ \AA}^{-1}$ ), while in the  $\bar{K}\bar{\Gamma}\bar{K}$  line it is deeper in energy.

Next we discuss the surface Dirac cone of  $\text{PbBi}_2\text{Te}_4$  in more detail by comparing it with other 3D TIs. The Dirac cone dispersion along  $\bar{\Gamma}\bar{M}$  and  $\bar{\Gamma}\bar{K}$  is shown in Fig. 2(a) for  $\text{PbBi}_2\text{Te}_4$  and for the well-studied TIs  $\text{Bi}_2\text{Se}_3$  and  $\text{TlBiSe}_2$ . Close to  $E_F$  the Dirac cone energy dispersion in  $\text{PbBi}_2\text{Te}_4$  is as steep as in the other materials, but it is apparently less steep near the Dirac point. In  $\text{PbBi}_2\text{Te}_4$ , the group velocity

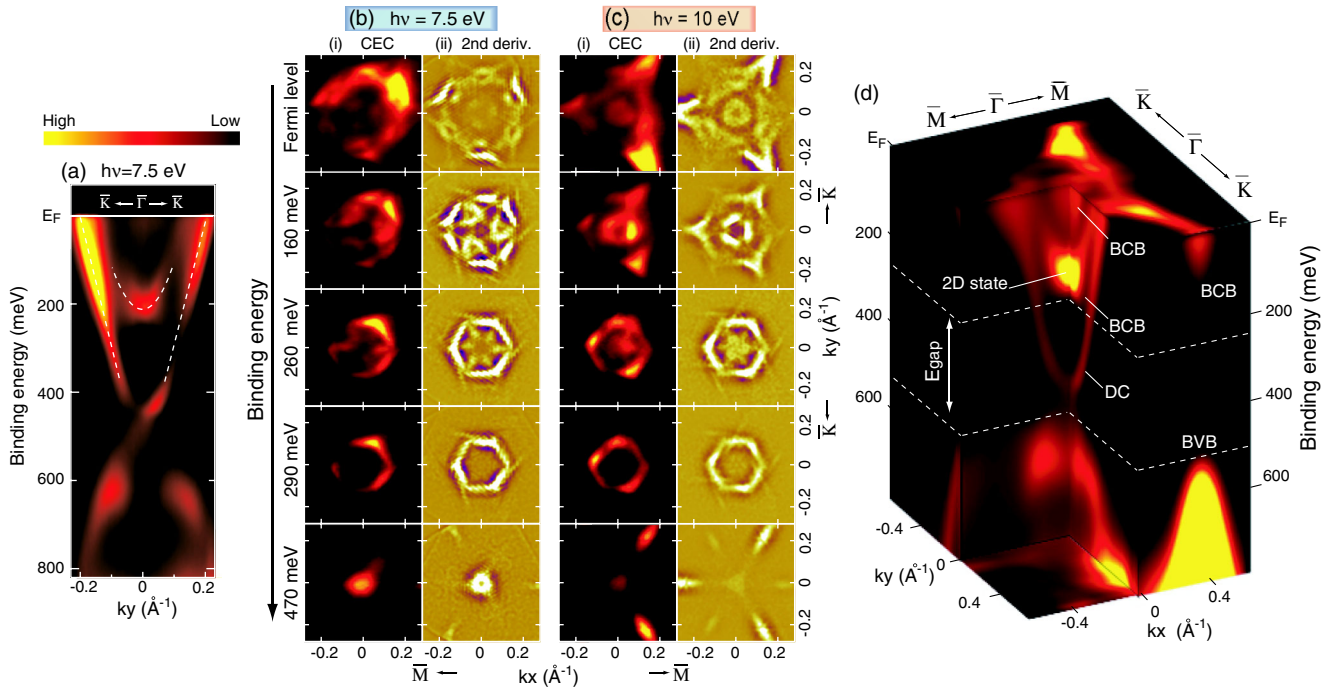


FIG. 1 (color online). (a) ARPES energy dispersion curves along the  $\bar{\Gamma}\bar{K}$  line acquired at  $h\nu = 7.5$  eV. Constant energy contour (CEC) maps (i) and their second derivatives (ii) obtained from the ARPES measurement at  $h\nu = 7.5$  eV (b) and 10 eV (c) in the  $\mathbf{k}_{\parallel}$  range  $-0.3 \text{ \AA}^{-1} \leq k_x, k_y \leq +0.3 \text{ \AA}^{-1}$  from  $E_B = 470$  meV (Dirac point) to 0 (Fermi level). The threefold symmetrization procedure is applied only for the second derivative images. (c) Three-dimensional map for  $h\nu = 10$  eV with Dirac cone (DC) surface state, two-dimensional parabolic band (2D state), BCB and BVB. The BCB bottom and BVB maximum separated by a bulk energy gap ( $E_{\text{gap}}$ ) are denoted with dashed lines.

at  $E_F$  is estimated as  $3.9 \times 10^5$  m/s, while near the Dirac point, it is much lower ( $1.4 \times 10^5$  m/s) than in  $\text{Bi}_2\text{Se}_3$  ( $2.9 \times 10^5$  m/s) [12] and in  $\text{TlBiSe}_2$  ( $3.9 \times 10^5$  m/s) [17]. The sizes of the isoenergy contours in the bulk energy gap from the Dirac point to 200 meV are much larger for  $\text{PbBi}_2\text{Te}_4$  than for the other two materials, as shown in Fig. 2(b). The estimated topological surface carrier density in  $\text{PbBi}_2\text{Te}_4$  obtained from the area of constant energy contour  $S(E)/4\pi^2$  is much larger than in the other two materials [Fig. 2(c)].

The theoretical bulk and surface band structures of  $\text{PbBi}_2\text{Te}_4$  are shown in Figs. 3(a) and 3(b), respectively. The calculations were performed with the VASP code [30,31] with optimized internal lattice parameters. In principle, three-dimensional materials with inversion symmetry are classified with four  $\mathbb{Z}_2$  topological invariants  $\nu_0$ ;  $(\nu_1\nu_2\nu_3)$ , which can be determined by the parity  $\xi_m(\Gamma_i)$  of occupied bands at eight time-reversal invariant momenta (TRIM)  $\Gamma_{i=(n_1,n_2,n_3)} = (n_1\mathbf{b}_1 + n_2\mathbf{b}_2 + n_3\mathbf{b}_3)/2$ , where  $\mathbf{b}_1, \mathbf{b}_2, \mathbf{b}_3$  are primitive reciprocal lattice vectors, and  $n_j = 0$  or 1 [1,2]. The  $\mathbb{Z}_2$  invariants are determined by the equations  $(-1)^{\nu_0} = \prod_{i=1}^8 \delta_i$  and  $(-1)^{\nu_k} = \prod_{n_k=1; n_j \neq k=0,1} \delta_{i=(n_1, n_2, n_3)}$ , where  $\delta_i = \prod_{m=1}^N \xi_{2m}(\Gamma_i)$  [2]. For rhombohedral lattice of  $\text{PbBi}_2\text{Te}_4$  the TRIMs are  $\Gamma, Z$ , and three equivalent  $L$  as well as  $F$  points [see SM [28], Fig. S1(b)]. The previous study confirmed that this compound is a strong topological insulator with the principal topological invariant  $\nu_0 = 1$  [27]. Here we analyze the  $(\nu_1\nu_2\nu_3)$  invariants. Interestingly, the parity inversion of bulk bands occurs at

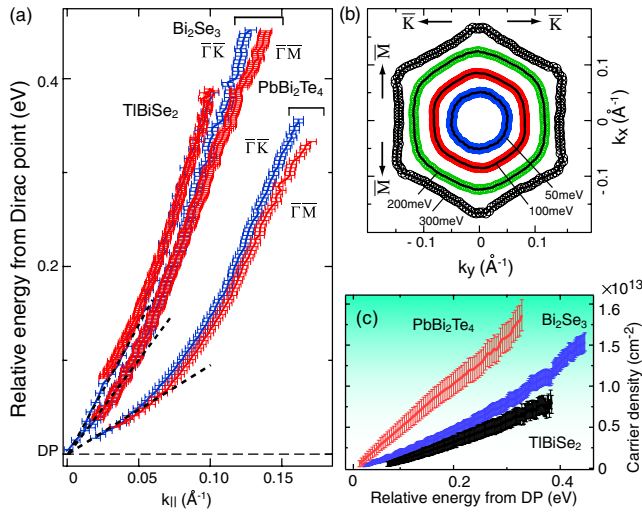


FIG. 2 (color online). (a) Experimental energy dispersion curves of surface Dirac cones along  $\Gamma\bar{M}$  and  $\Gamma\bar{K}$  lines in  $\text{PbBi}_2\text{Te}_4$  compared to  $\text{Bi}_2\text{Se}_3$  and  $\text{TlBiSe}_2$ . The curves are obtained from the intensity maxima of momentum distribution curves. The energy is relative to the Dirac point. (b) Constant energy contours for  $\text{PbBi}_2\text{Te}_4$ . (c) Estimated carrier densities  $S(E)/4\pi^2$  for three materials as a function of energy with respect to Dirac point (DP).  $S(E)$  is the area of the constant energy contour at energy  $E$ .

the  $Z$  point for  $\text{PbBi}_2\text{Te}_4$  [Fig. 3(a)], which leads to  $\mathbb{Z}_2$  invariants 1;(111). This is in contrast to the case of binary chalcogenides  $\text{Bi}_2\text{X}_3$  ( $X = \text{Se}, \text{Te}$ ), where the parity inversion takes place at the  $\Gamma$  point with  $\mathbb{Z}_2$  invariant 1;(000) [3]. Note that  $\text{PbBi}_2\text{Te}_4$  is the first case among the experimentally established topological insulators with  $\mathbb{Z}_2$  invariant 1;(111) possessing a single Dirac cone surface state. It is, thus, distinguished from the  $\text{Bi}_{1-x}\text{Sb}_x$  alloy with the same  $\mathbb{Z}_2$  invariant [32] but with 5 or 3 pairs of surface states crossing the Fermi energy [7,8]. In  $\text{Bi}_{1-x}\text{Sb}_x$ , owing to nonzero invariants  $(\nu_1\nu_2\nu_3)$ , a one-dimensional (1D) topologically protected state can exist at the dislocation core [33]. In the case of the layered crystal, the bulk dislocations can hardly exist, but other types of 1D TI states, such as edge states in thin films or 1D states at step edges, are possible.

Finally, we compare the experimental ARPES results with the theoretical band structures, see Fig. 3(b). The calculated band structure well reproduces the BCB minimum located at  $\bar{\Gamma}$  point at 200 meV above the Dirac point.

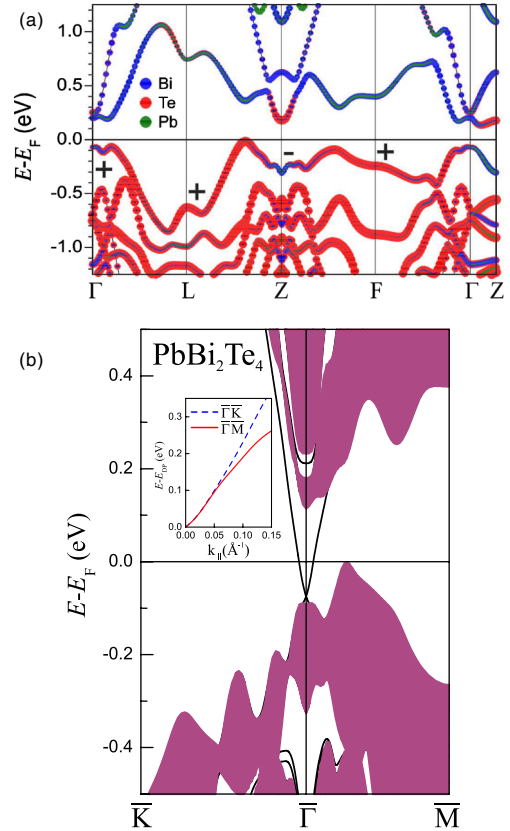


FIG. 3 (color online). (a) Bulk band structure of  $\text{PbBi}_2\text{Te}_4$  calculated along high symmetry directions of the Brillouin zone; colors show the weight of the states at Bi (blue), Te (red), and Pb (green) atoms, respectively. Signs of  $\delta_i = \pm 1$  at the TRIM are also shown. (b) Calculated surface (solid line) and bulk continuum states (shaded) of  $\text{PbBi}_2\text{Te}_4$  along  $\bar{K}\bar{\Gamma}\bar{M}$  line. The inset shows the surface Dirac cones in the limited momentum space for  $\bar{\Gamma}\bar{M}$  and  $\bar{\Gamma}\bar{K}$  lines.

Although the BVB maximum is higher in theory than in experiment, the theory well reproduces its location in  $\mathbf{k}$ -space, that is, it appears around  $1/3\bar{\Gamma}\bar{M}$  ( $k_{\parallel} \sim 0.3 \text{ \AA}^{-1}$ ). Anisotropic features along different symmetry lines can be recognized above 100 meV relative to the Dirac point, as depicted in the inset. In addition, the parabolic surface state appears at  $\sim 280$  meV above the Dirac point in the conduction band gap, which is consistent with the present observation (see SM [28], Fig. S3).

Our conclusion led by the present experiment is twofold: (i)  $\text{PbBi}_2\text{Te}_4$  is proved to be a three-dimensional topological insulator with the energy gap of 230 meV and a single Dirac cone at the  $\bar{\Gamma}$  point; (ii) the size of the Fermi surface contour in the bulk energy gap is significantly larger than in the other presently known 3D topological insulators, whereby the highest carrier density of the known topological surface states is achieved. These novel findings pave a way for the efficient control of the group velocity with sufficiently large spin current density by tuning the chemical potential in the bulk energy gap.

We thank Shuichi Murakami for valuable comments. We also thank J. Jiang, H. Hayashi, T. Habuchi, and H. Iwasawa for their technical support in the ARPES measurement at Hiroshima Synchrotron Radiation Center (HSRC). This work was financially supported by KAKENHI (Grants No. 20340092 and No. 23340105), Grant-in-Aid for Scientific Research (B) of JSPS. We also acknowledge partial support by the Department of Education of the Basque Country Government, the University of the Basque Country (project GV-UPV/EHU, Grant No. IT-366-07), Ministerio de Ciencia e Innovación (Grant No. FIS2010-19609-C02-00). Calculations were performed on SKIF-Cyberia (Tomsk State University) and Arina (UPV/EHU) supercomputers. The ARPES measurement was performed with the approval of the Proposal Assessing Committee of HSRC (Proposal No. 11-A-3 and 11-A-4). The SPring-8 experiments were carried out with the approval of the Japan Synchrotron Radiation Research Institute (JASRI) (Proposal No. 2010B0084, 2011A0084).

*Note added in proof.*—After submission, we became aware of an ARPES study of  $\text{Pb}(\text{Bi}_{1-x}\text{Sb}_x)_2\text{Te}_4$  by S. Souma et al. [34].

\*akiok@hiroshima-u.ac.jp

- [1] L. Fu, C.L. Kane and E.J. Mele, *Phys. Rev. Lett.* **98**, 106803 (2007).
- [2] L. Fu, and C.L. Kane, *Phys. Rev. B* **76**, 045302 (2007).
- [3] M.Z. Hasan and C.L. Kane, *Rev. Mod. Phys.* **82**, 3045 (2010).
- [4] X.L. Qi and S.C. Zhang, *Rev. Mod. Phys.* **83**, 1057 (2011).
- [5] Q. K. Xue, *Nature Nanotech.* **6**, 197 (2011).
- [6] F. Xiu, L. He, Y. Wang, L. Cheng, L. T. Chang, M. Lang, G. Huang, X. Kou, Y. Zhou, X. Jiang, Z. Chen, J. Zou, A. Shailos, and K.L. Wang, *Nature Nanotech.* **6**, 216 (2011).
- [7] D. Hsieh, Y. Xia, L. Wray, D. Qian, A. Pal, J.H. Dil, J. Osterwalder, F. Meier, G. Bihlmayer, C.L. Kane, Y.S. Hor, R.J. Cava, and M.Z. Hasan, *Science* **323**, 919 (2009).
- [8] A. Nishide, A.A. Taskin, Y. Takeichi, T. Okuda, A. Kakizaki, T. Hirahara, K. Nakatsuji, F. Komori, Y. Ando, and I. Matsuda, *Phys. Rev. B* **81**, 041309 (2010).
- [9] Y.L. Chen, J.G. Analytis, J.-H. Chu, Z.K. Liu, S.-K. Mo, X.L. Qi, H.J. Zhang, D.H. Lu, X. Dai, Z. Fang, S.C. Zhang, I.R. Fisher, Z. Hussain, and Z.-X. Shen, *Science* **325**, 178 (2009).
- [10] D. Hsieh, Y. Xia, D. Qian, L. Wray, F. Meier, J.H. Dil, J. Osterwalder, L. Patthey, A.V. Fedorov, H. Lin, A. Bansil, D. Grauer, Y.S. Hor, R.J. Cava, and M.Z. Hasan, *Phys. Rev. Lett.* **103**, 146401 (2009).
- [11] Y. Xia, D. Qian, D. Hsieh, L. Wray, A. Pal, H. Lin, A. Bansil, D. Grauer, Y.S. Hor, R.J. Cava, and M.Z. Hasan, *Nature Phys.* **5**, 398 (2009).
- [12] K. Kuroda, M. Arita, K. Miyamoto, M. Ye, J. Jiang, A. Kimura, E.E. Krasovskii, E.V. Chulkov, H. Iwasawa, T. Okuda, K. Shimada, Y. Ueda, H. Namatame, and M. Taniguchi, *Phys. Rev. Lett.* **105**, 076802 (2010).
- [13] R.C. Hatch, M. Bianchi, D. Guan, S. Bao, J. Mi, B.B. Iversen, L. Nilsson, L. Hornekær, and P. Hofmann, *Phys. Rev. B* **83**, 241303(R) (2011).
- [14] S. Kim, M. Ye, K. Kuroda, Y. Yamada, E.E. Krasovskii, E.V. Chulkov, K. Miyamoto, M. Nakatake, T. Okuda, Y. Ueda, K. Shimada, H. Namatame, M. Taniguchi, and A. Kimura, *Phys. Rev. Lett.* **107**, 056803 (2011).
- [15] S.V. Ereemeev, Yu.M. Koroteev, and E.V. Chulkov, *Pis'ma Zh. Eksp. Teor. Fiz.* **91**, 664 (2010) [*JETP Lett.* **91**, 594 (2010)].
- [16] S.V. Ereemeev, G. Bihlmayer, M. Vergniory, Yu.M. Koroteev, T.V. Menshikova, J. Henk, A. Ernst, and E.V. Chulkov, *Phys. Rev. B* **83**, 205129 (2011).
- [17] K. Kuroda, M. Ye, A. Kimura, S.V. Ereemeev, E.E. Krasovskii, E.V. Chulkov, Y. Ueda, K. Miyamoto, T. Okuda, K. Shimada, H. Namatame, and M. Taniguchi, *Phys. Rev. Lett.* **105**, 146801 (2010).
- [18] B. Yan, C.X. Liu, H.J. Zhang, C.Y. Yam, X.L. Qi, T. Frauenheim, and S.C. Zhang, *Europhys. Lett.* **90**, 37002 (2010).
- [19] H. Lin, R.S. Markiewicz, L.A. Wray, L. Fu, M.Z. Hasan, and A. Bansil, *Phys. Rev. Lett.* **105**, 036404 (2010).
- [20] T. Sato, K. Segawa, H. Guo, K. Sugawara, S. Souma, T. Takahashi, and Y. Ando, *Phys. Rev. Lett.* **105**, 136802 (2010).
- [21] Y.L. Chen, Z.K. Liu, J.G. Analytis, J.H. Chu, H.J. Zhang, B.H. Yan, S.K. Mo, R.G. Moore, D.H. Lu, I.R. Fisher, S.C. Zhang, Z. Hussain, and Z.X. Shen, *Phys. Rev. Lett.* **105**, 266401 (2010).
- [22] J.G. Analytis, J.H. Chu, Y. Chen, F. Corredor, R.D. McDonald, Z.X. Shen, and I.R. Fisher, *Phys. Rev. B* **81**, 205407 (2010).
- [23] K. Eto, Z. Ren, A.A. Taskin, K. Segawa, and Y. Ando, *Phys. Rev. B* **81**, 195309 (2010).

- [24] N.P. Butch, K. Kirshenbaum, P. Syers, A. B. Sushkov, G. S. Jenkins, H. D. Drew, and J. Paglione, *Phys. Rev. B* **81**, 241301 (2010).
- [25] S. V. Eremeev, Yu. M. Koroteev, and E. V. Chulkov, *Pis'ma Zh. Eksp. Teor. Fiz.* **92**, 183 (2010) [*JETP Lett.* **92**, 161 (2010)].
- [26] H. Jin, J. H. Song, A. J. Freeman, and M. G. Kanatzidis, *Phys. Rev. B* **83**, 041202 (2011).
- [27] T. V. Menshchikova, S. V. Eremeev, Yu. M. Koroteev, V. M. Kuznetsov, and E. V. Chulkov, *Pis'ma Zh. Eksp. Teor. Fiz.* **93**, 18 (2011) [*JETP Lett.* **93**, 15 (2011)].
- [28] See Supplemental Material at <http://link.aps.org/supplemental/10.1103/PhysRevLett.108.206803> for crystal growth procedure,  $h\nu$  dependence of the spectral intensity, experimental and theoretical band structures,  $k_z$  dependence of the bulk-derived state of  $\text{PbBi}_2\text{Te}_4$ .
- [29] L. E. Shelimova, O. G. Karpinskii, T. E. Svechnikova, E. S. Aivilov, M. A. Kretova, and V. S. Zemskov, *Neorg. Mater.* **40**, 1440 (2004) [*Inorg. Mater. (USSR)* **40**, 1264 (2004)].
- [30] G. Kresse and J. Furthmüller, *Comput. Mater. Sci.* **6**, 15 (1996).
- [31] G. Kresse and D. Joubert, *Phys. Rev. B* **59**, 1758 (1999).
- [32] J. C. Y. Teo, L. Fu, and C. L. Kane, *Phys. Rev. B* **78**, 045426 (2008).
- [33] Y. Ran, Y. Zhang, and A. Vishwanath, *Nature Phys.* **5**, 298 (2009).
- [34] S. Souma, K. Eto, M. Nomura, K. Nakayama, T. Sato, T. Takahashi, K. Segawa, and Y. Ando, *Phys. Rev. Lett.* **108**, 116801 (2012).